Disulfide Bond Structure of the AVR9 Elicitor of the Fungal Tomato Pathogen *Cladosporium fulvum*: Evidence for a Cystine Knot†

Henno W. van den Hooven,*,‡,|| Harrold A. van den Burg,‡ Paul Vossen,§ Sjef Boeren,‡ Pierre J. G. M. de Wit,§ and Jacques Vervoort*,‡

Laboratory of Biochemistry, Department of Biomolecular Sciences, Wageningen University, Dreijenlaan 3, 6703 HA Wageningen, The Netherlands, and Laboratory of Phytopathology, Department of Plant Sciences, Wageningen University, Binnenhaven 9, 6709 PD Wageningen, The Netherlands

Received October 3, 2000; Revised Manuscript Received January 9, 2001

ABSTRACT: Disease resistance in plants is commonly activated by the product of an avirulence (*Avr*) gene of a pathogen after interaction with the product of a matching resistance (*R*) gene in the host. In susceptible plants, *Avr* products might function as virulence or pathogenicity factors. The AVR9 elicitor from the fungus *Cladosporium fulvum* induces defense responses in tomato plants carrying the *Cf-9* resistance gene. This 28-residue β-sheet AVR9 peptide contains three disulfide bridges, which were identified in this study as Cys2−Cys16, Cys6−Cys19, and Cys12−Cys26. For this purpose, AVR9 was partially reduced, and the thiol groups of newly formed cysteines were modified to prevent reactions with disulfides. After HPLC purification, the partially reduced peptides were sequenced to determine the positions of the modified cysteines, which originated from the reduced disulfide bridge(s). All steps involving molecules with free thiol groups were performed at low pH to suppress disulfide scrambling. For that reason, cysteine modification by *N*-ethylmaleimide was preferred over modification by iodoacetamide. Upon (partial) reduction of native AVR9, the Cys2−Cys16 bridge opened selectively. The resulting molecule was further reduced to two one-bridge intermediates, which were subsequently completely reduced. The (partially) reduced cysteine-modified AVR9 species showed little or no necrosis-inducing activity, demonstrating the importance of the disulfide bridges for biological activity. Based on peptide length and cysteine spacing, it was previously suggested that AVR9 isa cystine-knotted peptide. Now, we have proven that the bridging pattern of AVR9 is indeed identical to that of cystine-knotted peptides. Moreover, NMR data obtained for AVR9 show that it is structurally closely related to the cystine-knotted carboxypeptidase inhibitor. However, AVR9 does not show any carboxypeptidase inhibiting activity, indicating that the cystine-knot fold is a commonly occurring motif with varying biological functions.

Surfaces and intercellular spaces of plants are continuously threatened by potential pathogens. However, only a few pathogens cause diseases in plants. In compatible interactions, a plant becomes diseased upon attack by a virulent pathogen, whereas in incompatible interactions, a plant is resistant to attack by a virulent pathogen. Disease resistance in plants commonly requires two complementary genes (gene-for-gene relationship) (*1*), an avirulence (*Avr*) gene in the pathogen and a matching resistance (*R*) gene in the host. An elicitor−receptor model has been proposed in which the pathogen-derived *Avr* products activate plant defense mechanisms upon *R*-protein-mediated recognition (e.g., *2, 3*). Pathogens secrete various proteins during interaction with plants. These proteins function as virulence or pathogenicity factors by modifying the host metabolism or by suppressing resistance mechanisms. It is suggested that plants produce *R*-proteins that detect proteinaceous molecules from invaders. The majority of the *R*-proteins contain leucine-rich repeats, which are expected to be involved in the detection of invading pathogens, either directly or indirectly (*4*). So far, little is known about possible virulence or pathogenicity functions of AVR proteins.

A well-studied example of a fungal avirulence protein is AVR9[1] (*5*), which is produced by particular races of *Cladosporium fulvum* when infecting its only natural host, the tomato. This 28-residue peptide induces a hypersensitive response in tomato plants carrying the resistance gene *Cf-9* (*6, 7*). This response is the most common plant resistance

* To whom correspondence should be addressed. Tel.: +31-317-482868. Fax: +31-317-484801. E-mail: Jacques.Vervoort@fad.bc.wau.nl or h.hooven@organon.oss.akzonobel.nl.

† This work was supported by an EC BIOTECH grant (BIO4-CT96-0515).

‡ Department of Biomolecular Sciences.

§ Department of Plant Science.

|| Present address: N.V. Organon, Department of Analytical Chemistry for Development, P. O. Box 20, 5340 BH Oss, The Netherlands.

[1] Abbreviations: AVR9^{3SS}/AVR9^{2SS}/AVR9^{1SS}/AVR9^{reduced}, AVR9 species with 3/2/1/0 disulfide bridges; *C. fulvum*, *Cladosporium fulvum*; CPI, carboxypeptidase inhibitor; 1D, one-dimensional; 3D, three-dimensional; IAM, iodoacetamide; MALDI-TOF MS, matrix-assisted laser desorption/ionization time-of-flight mass spectrometry; MM-Cf9, tomato genotype Moneymaker carrying the resistance gene *Cf-9*; NEM, *N*-ethylmaleimide; NOE, nuclear Overhauser enhancement; NOESY, NOE spectroscopy; ppm, parts per million; RP-HPLC, reversed-phase high-performance liquid chromatography; TCEP, tris-(2-carboxyethyl)-phosphine; TFA, trifluoroacetic acid; TOCSY, total correlation spectroscopy; 4VP, 4-vinylpyridine.

10.1021/bi0023089 CCC: $20.00
Published on Web 03/02/2001

response to viruses, bacteria, fungi, and nematodes (*2, 3, 8, 9*). AVR9 is a β-sheet peptide and contains three disulfide bridges (*10*). Mutagenesis studies revealed sites in AVR9 that are important for its necrosis-inducing activity (*10, 11*). All three disulfide bridges are required for this activity ((*11*) and this study).

The intrinsic function of AVR9 for the producing fungus is not known yet; however, the recognition of AVR9 by races of *C. fulvum* is clearly not the intrinsic function. Sequence homology could give a clue as to this function, but no close homologues were found in the sequence databases. It was noted that the length and the cysteine spacing of AVR9 are related to those of small cystine-knotted peptides (*10, 12*), which function as proteinase inhibitors or ion-channel blockers. Our NMR studies on AVR9 also suggested this relationship (*10*). However, in that study, the determination of a high-resolution 3D structure of AVR9 was hampered by the low amount of material and lack of information on the disulfide connectivities. Our recent folding studies on synthetic AVR9 (*13*) solved the first problem. Here, we report on the determination of the disulfide bridges of AVR9 to fully establish its relationship to cystine-knotted peptides, and to obtain significant input for NMR structure calculations to gain insight into the molecular mechanism mounting plant defense responses. In addition, a search for the intrinsic function of AVR9 was started with a comparison of AVR9 to the most closely related cystine-knotted peptide, the carboxypeptidase inhibitor (CPI) (*14*). However, AVR9 did not show any carboxypeptidase-inhibiting activity.

Disulfide bridges play important structural roles in proteins. The determination of the correct bridging pattern is not straightforward. A serious problem is disulfide scrambling, the exchange of partners between thiols and disulfides. This occurs at neutral or alkaline pH, but it can be suppressed at low pH (*15*). Different approaches have been applied to assign disulfide bridges. Classically, proteins are digested proteolytically, followed by characterization of the resulting fragments. Alternatively, partial hydrolysis can be used rather than proteolysis (e.g., *16*). Another method that is frequently used currently is partial reduction of disulfide bonds using tris-(2-carboxyethyl)phosphine (TCEP) (*17*). Advantages of this approach include the independence of accessible cleavage sites and minimization of disulfide scrambling using low-pH solutions. Using this reduction approach, we elucidated the bridging pattern of the cysteine-rich AVR9 (six cysteines out of 28 residues).

MATERIALS AND METHODS

Materials. Folded synthetic AVR9, proven to be identical to native fungal AVR9, was obtained as described previously (*13*). TCEP was from Sigma. *N*-ethylmaleimide (NEM) and 4-vinylpyridine (4VP) were purchased from Fluka. Iodoacetamide (IAM), potato carboxypeptidase inhibitor, bovine pancreas carboxypeptidase A, and benzoylglycyl-L-phenylalanine were obtained from ICN Biomedicals Inc. All solvents were HPLC grade. The 4VP was vacuum distilled and kept under nitrogen at −70 °C.

Partial Reduction. Native AVR9 (36 μg, MW 3189.6) was dissolved in 10 μL of 0.1 M citrate buffer, pH 3, containing 6 M guanidine hydrochloride in water. Reduction was started by adding the appropriate amount of an aqueous solution containing 0.1 M TCEP, 0.1 M citrate, pH 3, and 6 M guanidine−HCl. In most cases, 240 equiv of TCEP (mole TCEP to mole AVR9) was added (27.2 μL of TCEP solution). This partial-reduction mixture was incubated at room temperature for 15 min (unless stated otherwise), directly followed by alkylation or HPLC analysis. HPLC fractions, containing partially reduced peptides, were collected manually, and the masses of the corresponding peptides were determined by MALDI-TOF MS.

Alkylation with Iodoacetamide. Partially reduced AVR9 (see above) in 37.2 μL of 0.1 M citrate, pH 3, 6 M guanidine−HCl in water, with 240 equiv TCEP was alkylated with iodoacetamide as described previously (*17*). For one reaction 20−40 mg of IAM was used. After incubation for 30 s at room temperature, the reaction was quickly acidified with phosphoric acid (85%) to prevent disulfide scrambling. This mixture was immediately applied to the HPLC column.

Alkylation with N-Ethylmaleimide. To the mixture after partial reduction of AVR9 (240 equiv of TCEP, 15 min) was added 68 μL of 0.1 M *N*-ethylmaleimide (600 equiva), 0.1 M citrate, pH 3, and 6 M guanidine−HCl in water. After incubation for 30 min at room temperature, the mixture was directly applied to the HPLC column.

Alkylation with 4-Vinylpyridine. Only fully reduced peptides were alkylated with 4-vinylpyridine (*17*). Complete reduction was obtained by incubation of freeze-dried HPLC-purified peptides in 200 μL of an aqueous solution containing 20 mM TCEP and 250 mM Tris-acetate, pH 8, for 30 min at 50 °C. After the solution cooled to room temperature, 4 μL of neat colorless 4VP was added. The mixture was incubated for 15 min in the dark at room temperature, immediately followed by addition of 20 μL of 85% phosphoric acid and HPLC purification.

Reversed-Phase High-Performance Liquid Chromatography. Different disulfide forms of AVR9 were separated by analytical RP-HPLC. The elution solvents consisted of 5% acetonitrile (v/v) and 0.1% trifluoroacetic acid (TFA) in water (solvent A), and 10% water and 0.1% TFA in acetonitrile (solvent B). A 150 × 3.9 mm Delta-Pak C_{18} column (300 Å, 5 μm) (Waters Corp., Milford, MA) was used. The separation was monitored at 215 nm, with a flow rate of 1 mL/min. The gradient used to analyze reaction mixtures was 0−12% B in 7 min (percentage solvent B in solvent A), 12−37% B in 33 min, giving a total time of 40 min. Relative amounts of different disulfide forms of AVR9 were determined by integrating the appropriate peaks in the analytical HPLC profiles using standard Waters software.

Peptide Sequence Analysis. Automated Edman degradation, using a Perkin-Elmer/Applied Biosystems model 476A, was performed at the Sequence Center Utrecht (University of Utrecht, The Netherlands). The sequencer was on-line connected to an RP-HPLC for the identification of the phenylthiohydantoin derivatives of the released amino acids.

Assay of Necrosis-Inducing Activity. Injections of peptides (20 μL) into the intercellular space of leaves of tomato cultivars MM-Cf9 (containing the *Cf-9* resistance gene) and MM-Cf0 (lacking the *Cf-9* gene) were carried out as described previously (*11, 18*).

Assay of Carboxypeptidase Inhibitor Activity. The K_i values of the carboxypeptidase inhibitor and of AVR9 were determined according to the method described by Henderson

(*19*). Benzoylglycyl-L-phenylalanine was used as substrate at different concentrations, as previously reported (*20*). The concentration of carboxypeptidase A was 67 nM in all cases.

Mass Spectrometry. Average molecular masses were determined by MALDI-TOF MS on a Perseptive Biosystems Voyager DE-RP. A saturated matrix solution (α-cyano-4-hydroxycinnamic acid, Aldrich) was freshly prepared in acetonitrile/water/TFA (50/50/1, v/v/v). One microliter of each protein sample (freeze-dried HPLC fractions, dissolved in 10 μL of water) was mixed with 1 μL of matrix solution on the MALDI target. Data were acquired in the positive reflector mode. External calibration was performed with a tryptic digest of the C116S mutant of p-hydroxybenzoate hydroxylase (EC 1.14.13.2) using fragments with calculated $[M + H]^+$ values of 1099.6 and 2086.2.

NMR Spectroscopy. The sample contained 5 mg of native AVR9 in 0.2 mL of $H_2O/^2H_2O$ (9:1 v/v) at pH 5.0 (pH meter reading) and was transferred to a Shigemi tube (Shigemi Inc., Allison Park, PA). Experiments were conducted at 35 °C. 1D-NMR spectra, a clean MLEV17-TOCSY spectrum with a mixing time of 50 ms, and a NOESY spectrum with a mixing time of 300 ms were recorded at 500 MHz on a Bruker AMX500 NMR spectrometer. Acquisition and processing parameters were essentially the same as those described previously (*10*). The spectra were referenced to sodium 3-(trimethylsilyl)-1-propanesulfonate (DSS).

RESULTS

The determination of the disulfide bridge structure of AVR9 involved four steps: (1) partial reduction, (2) alkylation of the free thiol groups of newly formed cysteines, (3) separation of different peptides by HPLC, and (4) Edman degradation of peptides to locate the positions of the alkylated cysteines.

Partial Reduction of AVR9. Native AVR9 was reduced by TCEP. This water-soluble reagent has proven to be an excellent reducing agent for disulfides (*21*), and can be used at acidic pH to suppress disulfide scrambling (*17*, *22*). The reduction reactions (at pH 3) were performed in 6 M guanidine−HCl to facilitate equal TCEP accessibility to the three disulfide bridges of AVR9. A partial reduction typically yielded five different AVR9 species, as can be seen in the HPLC profile presented in Figure 1A. MALDI-TOF MS demonstrated that one of these species contained three bridges ($AVR9^{3SS}$), one contained two bridges ($AVR9^{2SS}$), two contained one bridge ($AVR9^{1SS}$), and one contained no bridges ($AVR9^{reduced}$) (Figure 1A). The retention time on HPLC and the biological activity of the $AVR9^{3SS}$ species are identical to those of native AVR9. Thus, next to native and fully reduced AVR9, three partially reduced AVR9 species were obtained. The three disulfide bridges of AVR9 could be assigned on the basis of the three partially reduced species obtained, as demonstrated below. The amount of TCEP in the reaction mixture (Figure 1B) and the incubation time (Figure 1C) affect the reduction rate and the yields of the different disulfide forms. Relatively high concentrations of TCEP are required to obtain significant quantities of the partially reduced AVR9 molecules (Figure 1B). The presence of guanidine−HCl in the TCEP solution somewhat decreased the yields of $AVR9^{2SS}$, $AVR9^{1SS}$, and $AVR9^{reduced}$. In time, as expected, a $AVR9^{2SS}$ species appeared first, followed after a short lag time by two $AVR9^{1SS}$ species, and finally the $AVR9^{reduced}$ species (Figure 1C). The amount of $AVR9^{reduced}$ increased slowly in the first 10 min, but increased strongly after 15 min, when significant amounts of $AVR9^{1SS}$ became available. This phenomenon can also be observed in the TCEP titration experiment (Figure 1B). The data presented in Figure 1 suggest that AVR9 is sequentially reduced as follows: $AVR9^{3SS} \rightarrow AVR9^{2SS} \rightarrow AVR9^{1SS} \rightarrow AVR9^{reduced}$. In the subsequent alkylation reactions, partial-reduction mixtures were used that were obtained after 15 min of incubation with 240 equiv of TCEP.

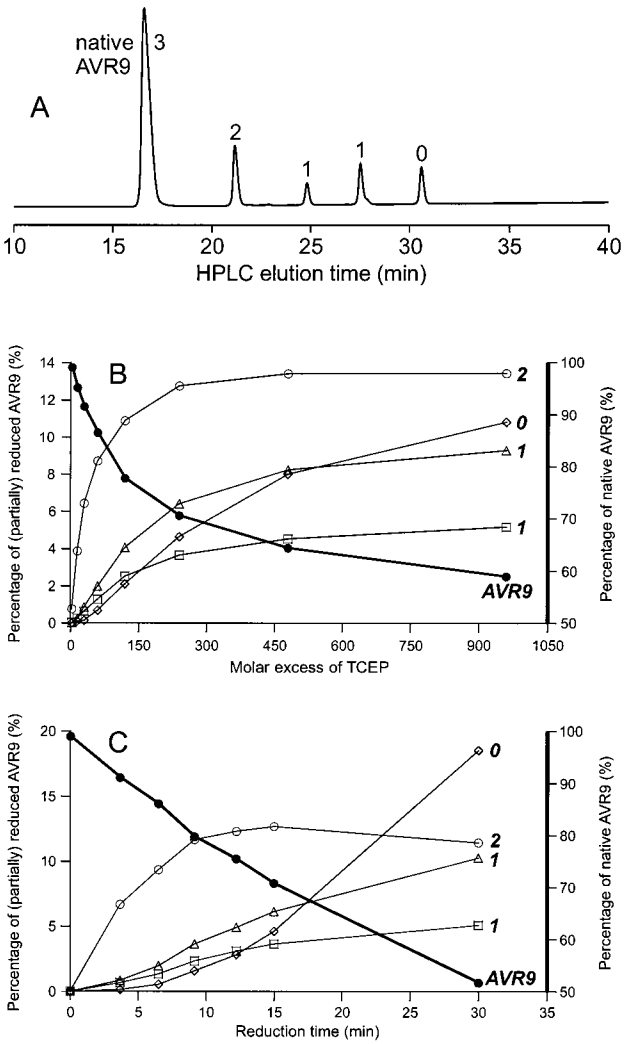

FIGURE 1: Partial reduction of AVR9. (A) HPLC profile (monitored at 215 nm) of a partial reduction reaction of native AVR9 in 6 M guanidine−HCl, pH 3, with a 240-fold molar excess of TCEP, at room temperature for 15 min. For every peak the number of disulfide bridges present in the corresponding AVR9-derived species is indicated. The peak at 17 min represents native AVR9. (B) Relative amounts of native AVR9 and (partially) reduced AVR9 species as a function of the molar excess of TCEP (other conditions as stated above, reaction time 15 min). The percentages were determined by integration of the corresponding HPLC profiles. (C) Partial reduction as function of time (other conditions as stated above, 240-fold excess of TCEP).

Iodoacetamide Labeling of Partially Reduced AVR9. In the originally proposed strategy (*17*), IAM was used to irreversibly block the thiol groups of the cysteines formed during partial reduction. This reagent alkylates at pH 8. The partial-reduction mixture, containing 6 M guanidine−HCl, was squirted into a concentrated IAM solution and was

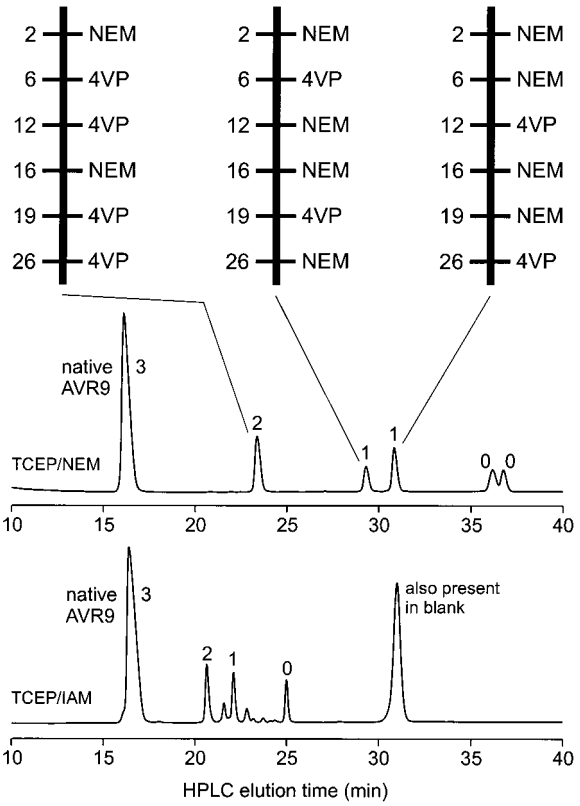

FIGURE 2: HPLC profiles of partially reduced and cysteine-modified AVR9, and the positions of those cysteine modifications. Native AVR9 was partially reduced for 15 min by a 240-fold molar excess of TCEP, at room temperature, pH 3, and 6 M guanidine−HCl. The reaction mixture was analyzed by HPLC after treatment with IAM (bottom HPLC profile) or with NEM (top HPLC profile). The numbers of disulfide bridges present in AVR9 derivatives in various peaks are indicated. In the profile of the TCEP/IAM reaction, a peak was observed at 31 min that was not related to AVR9. This peak was the only one present in a control reaction without AVR9. The partially reduced NEM-modified peptides were collected, lyophilized, and fully reduced by TCEP followed by modification of free cysteines by 4-vinylpyridine. The positions of the modifications, as determined by Edman degradation, are shown in the top panel.

quenched after 30 s by acidification. The resulting mixture was directly applied to the HPLC column. The number of peaks in the resulting HPLC profile (Figure 2) exceeded that observed after partial reduction without alkylation (Figure 1A). The peak with a retention time of 31 min in Figure 2 (TCEP/IAM) was also seen in a control experiment with TCEP/IAM without the peptide. Native AVR9 was not modified by IAM and showed the expected HPLC retention time of 17 min. Analysis by MS demonstrated that all other peaks contained AVR9 species alkylated on all free cysteines (AVR9[IAM]), depending on the number of disulfide bridges left in the molecule. The additional peaks, formed during treatment with IAM, contain AVR9-related species with one or two bridges and four or two *S*-carboxamidomethylcysteine residues, respectively. These species were caused by disulfide scrambling during alkylation. The three most intense peaks eluting between 20 and 25 min (numbered in Figure 2, TCEP/IAM) correspond to peaks observed after partial reduction without alkylation ($AVR9^{2SS}$, most abundant $AVR9^{1SS}$, and $AVR9^{reduced}$; Figure 1A). The less abundant $AVR9^{1SS}$ peak observed after partial reduction (Figure 1A) could not be recognized with certainty after alkylation. $AVR9^{2SS}$[IAM] and the most abundant $AVR9^{1SS}$[IAM] peptide were sequenced.

Partial reduction of the small cysteine-rich AVR9 peptide results in free thiol groups, which are always in the vicinity of the remaining disulfides, thereby favoring scrambling. The presence of 6 M guanidine−HCl in the TCEP solution somewhat reduced the level of scrambling. Attempts to alkylate the partially reduced AVR9 species after HPLC purification did not further reduce the level of scrambling.

N-Ethylmaleimide Labeling of Partially Reduced AVR9. Alkylation with NEM was carried out for 30 min at pH 3 by adding 600 molar equiv NEM, directly after partial reduction. This reaction was complete as evidenced by mass spectrometry, whereas lower amounts of NEM resulted in incomplete alkylation. HPLC analysis of the reaction mixture (Figure 2; TCEP/NEM) showed the absence of disulfide scrambling. The AVR9 species present after partial reduction (Figure 1A) are all recognized after alkylation with NEM (Figure 2). The AVR9[NEM] derivatives showed increased HPLC retention times, in comparison with the corresponding (partially) reduced AVR9 species. However, $AVR9^{reduced}$-[NEM] shows two HPLC peaks (both marked "0"). MALDI-TOF MS showed that the AVR9-related species in the latter two peaks have identical masses. The peaks of $AVR9^{reduced}$-[NEM] were collected separately, freeze-dried, and analyzed again by HPLC. No redistribution in the two peaks was observed, indicating that the two AVR9 derivatives are not in a conformational equilibrium. Multiple peaks after NEM labeling have been observed before (*23*, *24*), and probably represent diastereoisomers, caused by the attack of a thiol group to the maleimide introducing a new chiral center, or ring opening of the *N*-ethylsuccinimidocysteines.

Sequencing of AVR9 Peptides with Labeled Cysteines. The two partially reduced IAM-labeled peptides (Figure 2; TCEP/IAM, labeled 1 and 2) still contain one or two disulfide bridges. Cysteine residues involved in these bridges do not give a signal during peptide sequencing, whereas *S*-carboxamidomethylcysteines give clearly identifiable signals. As the sequence of AVR9 is known, only the cycles concerning cysteine-derived residues give relevant information. In all cases, the signals of the non-cysteine-derived residues were in perfect agreement with the known sequence. Edman degradation of the $AVR9^{2SS}$[IAM] peptide revealed signals due to *S*-carboxamidomethylcysteines in cycles 2 and 16, and the absence of signals in cycles 6, 12, 19, and 26. Thus, the first-opened disulfide bridge connects residues Cys2 and Cys16. The $AVR9^{1SS}$[IAM] peptide, unfortunately, did not show two cycles where signals were clearly absent, although the signals observed in cycles 12 and 26 were the lowest. No disulfide connectivity could be deduced with certainty from this experiment. Possibly, the HPLC-purified peptide was contaminated with disulfide-scrambled AVR9 species, blurring the difference between the absence and the presence of *S*-carboxamidomethylcysteine signals. Discrimination will be easier when the remaining bridge(s) is (are) reduced and the newly formed cysteines are modified by another label. The IAM-modified peptides were more difficult to purify than the NEM-modified ones (Figure 2).

The three partially reduced NEM-labeled AVR9 peptides were purified by HPLC (Figure 2), freeze-dried, completely reduced, and treated with 4VP. The resulting linear peptides contained NEM- and 4VP-labeled cysteines, which were

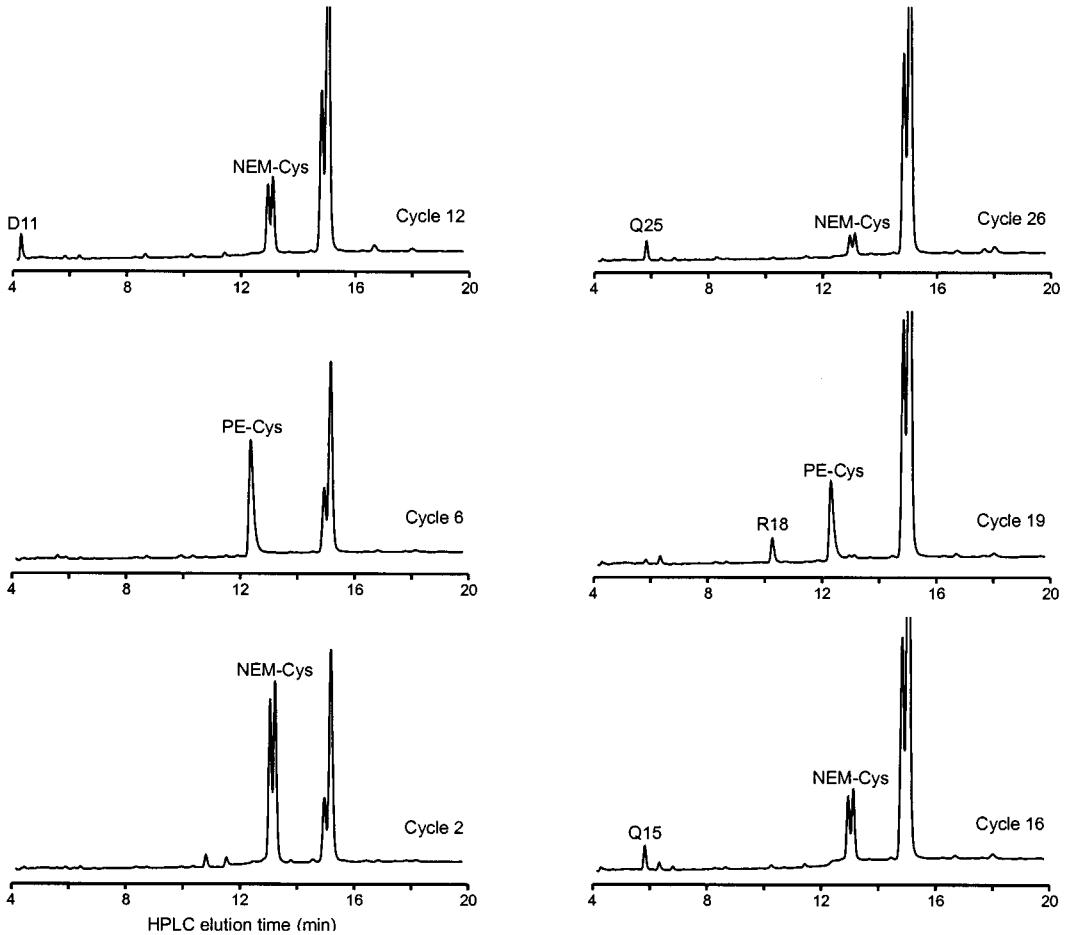

FIGURE 3: HPLC profiles of Edman-sequencing cycles corresponding to the release of modified cysteines from the first-eluting AVR9^{1SS}-[NEM,4VP] peptide. Native AVR9 was partially reduced to AVR9^{1SS} (HPLC peak at 25 min in Figure 1). The four newly formed cysteines were modified by NEM (AVR9^{1SS}[NEM], HPLC peak at 29 min in Figure 2). Subsequently, the remaining bridge was reduced, and those two cysteines were modified by 4VP. The resulting peptide was sequenced, and the signals of the phenylthiohydantoin derivatives of the released modified cysteines in the cycles 2, 6, 12, 16, 19, and 26 are shown. Signals of cysteines modified by *N*-ethylmaleimide are indicated by "NEM-Cys", and those of pyridylethylated cysteines (4VP) by "PE-Cys". A disulfide bridge between the residues Cys6 and Cys19 is deduced from these data. The signals of the preceding amino acid in the sequence observed in the cycles 12, 16, 19, and 26 are indicated by the one-letter code of those residues (D11, Q15, R18, and Q25, respectively). Two chemical byproducts elute in the HPLC chromatograms at about 15 min.

easily observed and identified during sequencing. The phenylthiohydantoin derivative of NEM-labeled cysteine eluted as two peaks (Figure 3). Multiple peaks for this residue have been observed before (*23*−*25*). This may be related to hydrolysis of the maleimide ring, or to the introduction of a chiral center upon NEM labeling. Sequencing of the 4VP-treated, fully reduced AVR9^{2SS}[NEM] peptide (AVR9^{2SS}-[NEM,4VP]) yielded signals corresponding to NEM-Cys in cycles 2 and 16, and signals of pyridylethylcysteine (PE-CYS) in cycles 6, 12, 19, and 26 (results summarized in Figure 2). These data confirm the existence of a disulfide bridge between the residues Cys2 and Cys16 in native AVR9, as was deduced from the sequencing of the AVR9^{2SS}[IAM] peptide. The first-eluting AVR9^{1SS}[NEM,4VP] peptide showed PE-CYS signals in cycles 6 and 19 (Figure 3), whereas the last-eluting AVR9^{1SS}[NEM,4VP] peptide displayed these signals in cycles 12 and 26. The other four cysteines of both peptides all appeared modified by NEM. In summary, disulfide bridges connect the residues 2 and 16, 6 and 19, and 12 and 26. The primary structure of native AVR9 including the bridging pattern is shown in Figure 4.

Necrosis-Inducing Activities of Partially Peduced NEM-Labeled AVR9 Species. The NEM-modified peptides, at various concentrations, were injected into the leaves of MM-Cf9 tomato plants to determine the necrosis-inducing activities (shown in Table 1). Native AVR9 showed full activity, AVR9^{2SS}[NEM] displayed strongly reduced activity, and peptides with one or no bridges were not active at all. Reduced AVR9 with free thiol groups showed a very low necrosis-inducing activity at the highest concentration. This is likely due to some refolding in the intercellular space of tomato leaves. None of the injections in MM-Cf0 plants showed necrosis-inducing activity (result not shown).

FIGURE 4: Primary structure and disulfide bonding pattern of AVR9. The disulfide bridges are indicated, and the cysteine residues are numbered.

NMR Analysis of AVR9. Based on the length, cysteine spacing, and disulfide connectivities AVR9 belongs to the family of cystine-knotted peptides, such as the ω-conotoxins (Figure 5). A strong homology is observed to carboxypeptidase inhibitor (CPI). To prove the structural homology,

Table 1: Necrosis-Inducing Activities[a] of Native AVR9, (Partially) Reduced NEM-Modified AVR9 Species, and Fully Reduced AVR9 as Observed upon Injection in Leaves of MM-Cf9 Tomato Plants

AVR9 species[b]	concentration		
	30 μM	3 μM	0.3 μM
native AVR9	+ + + + + +	+ + + +	+ +
AVR9^{2SS}[NEM](6−19,12−26)	+	−	−
AVR9^{1SS}[NEM](6−19)[c]	−	−	−
AVR9^{1SS}[NEM](12−26)[d]	−	−	−
AVR9^{0SS}[NEM][e]	−	−	−
AVR9^{0SS}[NEM][f]	−	−	−
AVR9^{0SS}	+	−	−

[a] Necrosis-inducing activities are qualified as reported previously (*11*). [b] The numbers of disulfide bridges in the molecules are indicated. Cysteine thiol modifications by *N*-ethylmaleimide (NEM) and the remaining disulfide bridges (SS) in the partially reduced AVR9 species are also indicated. [c] RP-HPLC peak at 29 min (Figure 2, top chromatogram). [d] RP-HPLC peak at 31 min (Figure 2, top chromatogram). [e] First-eluting on RP-HPLC at 36 min (Figure 2, top chromatogram). [f] Last-eluting on RP-HPLC at 37 min (Figure 2, top chromatogram).

```
AVR9          YC---NSSCTRAF-DC--LGQCGRCDFHKLQCVH
CPI IIb    <EEHADPIC---NKPCKTHD-DCSGAWFCQACWNSARTCGPYVG
Kalata B1     NGLPVC---GETCVGGT--CNTPG-C-TCSWP--VCTR
CMTI I          RVCPRILMECKKDS-DC--LAEC-VCLEH-GYCG
ω-GVIA           CKSOGSSCSOTSYNC-----CRSCNOYTKRCY
```

FIGURE 5: Alignment of amino acid sequences of the cystine-knotted peptides AVR9, carboxypeptidase inhibitor IIb (CPI IIb) (*27*), Kalata B1 (*12, 30*), trypsin inhibitor CMTI I (*40*), and ω-conotoxin GVIA (*41*). Cysteines involved in disulfide bridges are indicated in bold. The bridging patterns in these molecules are identical. The residue hydroxyproline in the ω-conotoxin GVIA is indicated by O. The N-terminal residue in CPI IIb is a pyroglutamate, which is indicated by <E.

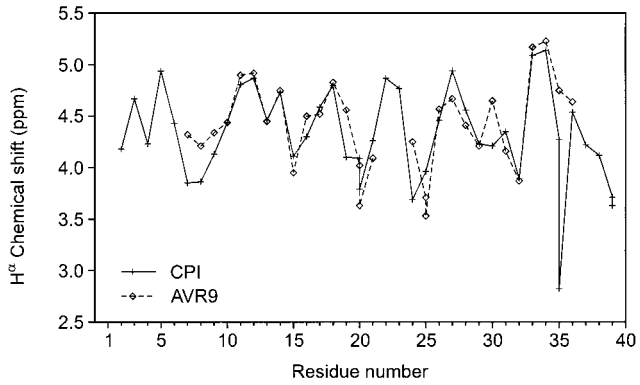

FIGURE 6: Comparison of H$^{\alpha}$-proton chemical shifts of AVR9 and carboxypeptidase inhibitor. H$^{\alpha}$ chemical shifts (ppm) are shown versus the residue number for CPI (+, solid line), and for AVR9 (◊, dashed line). The data for CPI were derived from NMR spectra recorded at 35 °C and pH 3.8 (*26*), and the data for AVR9 from spectra taken at 35 °C and pH 5. The residues of AVR9 are superimposed (and numbered) onto the corresponding ones of CPI (Figure 5).

NMR spectra were recorded for AVR9 at the temperature at which the NMR spectra of CPI had been obtained (*26*). The resonances of AVR9 at 35 °C were assigned on the basis of those obtained for the peptide at room temperature and 5 °C (*10, 13*). No significant differences were observed between these three data sets. The backbone H$^{\alpha}$-proton chemical shifts of AVR9 at 35 °C and pH 5 are depicted in Figure 6, together with those obtained for CPI (35 °C and pH 3.8, *26*). Strong similarities are observed between the shifts of AVR9 and CPI despite the large differences in the amino acid sequence, indicating a comparable fold.

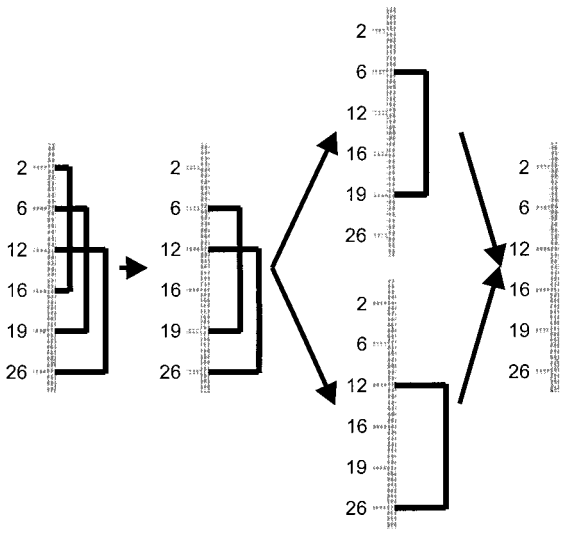

FIGURE 7: Scheme of the reduction of AVR9 by TCEP. The peptide sequence is represented by a gray line. Only the positions of the six cysteines are indicated. The disulfide bridges in the different molecules are shown by connections between the cysteines involved. If not connected, cysteines have free sylfhydryl groups.

Testing Possible Carboxypeptidase-Inhibiting Activity of AVR9. To determine whether a common fold would still lead to common functions, and to study the intrinsic function of AVR9 for the producing fungus, the possibility was investigated whether AVR9 would have biological activities similar to those of its most closely related peptide. First, the competitive inhibitory activity of the carboxypeptidase inhibitor toward carboxypeptidase A was determined. The inhibition constant K_i of 2.1 nM is in perfect agreement with previously reported values of 1.5−2.7 nM (*27*) and 0.9−2.1 nM (*20*). However, inhibition of carboxypeptidase was not observed with AVR9. Even an AVR9 concentration 1000-fold higher than that of CPI did not inhibit carboxypeptidase A.

DISCUSSION

The fungal AVR9 elicitor is secreted in the intercellular space of tomato leaves, and it is likely to require additional stability, for which purpose disulfide bridges are ideally suited. The disulfide connectivities have now been identified as Cys2−Cys16, Cys6−Cys19, and Cys12−Cys26 (Figure 4). These overlapping disulfide bridges are envisioned to increase the stability of the peptide.

The applied "partial-reduction procedure" worked out well for AVR9, despite the high cysteine content (six "half-cystines" out of 28 residues). For this procedure sufficient accessibility of the sulfur atoms of at least one bridge is required. In this respect, it is noted that the bridging rendered AVR9 insensitive toward trypsin and chymotrypsin (*6*), complicating a determination of disulfide connectivities by proteolytic digestions. In general, these digestions are performed at a pH that does not suppress disulfide scrambling. The high cystine content also complicated an NMR spectroscopic approach to determining the bridging pattern, as was also observed for some related (vide infra) cystine-rich peptides (*28*−*30*). This suggests that the partial-reduction procedure is an attractive approach for highly bridged peptides.

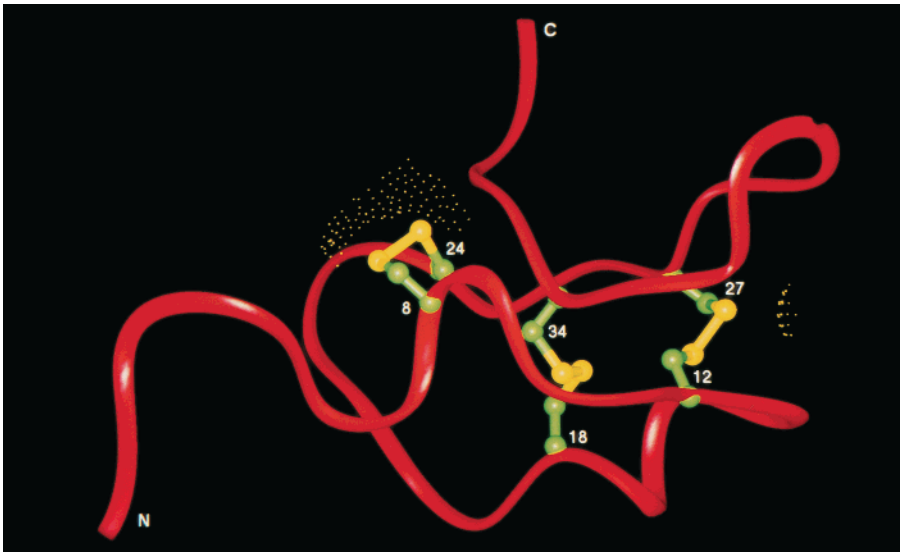

FIGURE 8: Solvent-accessible surface of the sulfur atoms in the carboxypeptidase inhibitor. The coordinates of CPI are taken from the crystal structure of the inhibitor complex of carboxypeptidase A (*42*). The backbone of CPI is indicated as a solid red ribbon with labeled termini. Cysteine side chains are depicted in a ball-and-stick representation with their numbers in the sequence. The solvent-accessible surfaces of the sulfur atoms are indicated by yellow dots. Only the bridge Cys8−Cys24 is sufficiently accessible to a molecule of the size of TCEP.

In the course of the reduction of AVR9, only the bridge between Cys2 and Cys16 opened. This intermediate was further reduced to two AVR9^{1SS} species (Figure 1), which were subsequently reduced completely. The reduction pathway is depicted in Figure 7. In general, multiple intermediates with one opened bridge are used to deduce the bridging. However, intermediates with one bridge left can be used equally well as demonstrated for AVR9. Though reduction was performed in the presence of 6 M guanidine−HCl to lessen possible differences in the accessibility of TCEP to each disulfide bond, only the Cys2−Cys16 bridge in the intact molecule is sufficiently accessible to TCEP. A relatively high TCEP concentration was required for partial reduction of AVR9 when compared to the required concentrations for other proteins (*17*, *22*). From these data, qualitative information on the spatial structure of AVR9 is obtained. The sulfur atoms of two bridges are buried in AVR9, and those of the Cys2−Cys16 bridge are partially shielded within the molecule. The molecule is rather stable under denaturing conditions.

Iodoacetamide was used first for the labeling of the cysteines formed during partial reduction, as originally proposed (*17*). Unfortunately, disulfide scrambling, also reported by Gray (*17*), was significant during this modification. As a result, the low-intensity AVR9^{1SS}[IAM] intermediate got lost (Figures 1 and 2). One of the two remaining partially reduced IAM-modified peptides gave clear results after sequencing, whereas the other peptide gave signals that could hardly be differentiated for IAM-modified cysteines and "blank" half-cystines. One way to improve this is to reduce the remaining bridges and label the resulting cysteines with a different agent. Contrary to the case when using iodoacetamide, no scrambling was observed during modification with *N*-ethylmaleimide at the low pH at which the partial reduction was performed. The remaining bridges of the purified AVR9^{2SS}[NEM] and AVR9^{1SS}[NEM] intermediates were reduced, followed by modification with 4-vinylpyridine. Sequencing revealed the positions of the modifications, as the signals originating from Cys(NEM) and Cys(4VP) are clearly different (Figure 3). Labeling with NEM rather than with IAM was essential for the elucidation of the bridging of AVR9. The compatibility of the low-pH partial reduction and modification with NEM is probably also useful for the determination of disulfide bridges in other peptides as well, because of substantially less disulfide scrambling. An alternative agent to alkylate cysteines under acid catalysis is (hydroxymethyl)benzamide in TFA (*31*), but this reagent is less compatible with TCEP. For larger proteins, the TCEP/NEM approach can be combined with proteolytic digestions (*23*). Alternatively, cysteines, formed by partial reduction, can be cyanylated at low pH allowing cleavage of the N-terminal peptide bond followed by mass mapping (*22*). This cyanylation approach may in the cases of (poly)peptides yield very small fragments that might escape detection by MALDI-TOF MS because of interference with signals arising from the matrix.

The necrosis-inducing activity of AVR9 strongly decreased upon reduction of the Cys2−Cys16 disulfide bond. Further reduction inactivated the molecules completely. Thus, the bridges are very important for the activity of AVR9, which is in perfect agreement with mutagenesis studies (*11*). Most likely the drop in activity is caused by reduced stability and/or loss of native conformation, suggesting that at least the Cys2−Cys16 bridge is required for a stable native spatial structure. It is noted that in the case of the related cystine-knotted ω-conotoxins, each of the three bridges plays an essential role in stabilizing the structure (*32*). The strongly reduced necrosis-inducing activity of the AVR9^{2SS} molecule, which has the only accessible bridge reduced, does not favor a mechanism involving the formation of a disulfide bridge between AVR9 and a (co)receptor in the tomato.

The search for an intrinsic function of AVR9 for *C. fulvum* was initiated by examining homologous peptides. No proteins with high sequence identity to AVR9 could be found. However, based on length, cysteine spacing (Figure 5), and β-sheet character, homology to inhibitor cystine-knotted peptides was suggested (*10*, *12*). AVR9 is most homologous to the CPI (Figure 5). The present study shows that the

bridging of AVR9 is identical to that of the cystine-knotted peptides. Also, the backbone H^{α}-proton chemical shifts of AVR9 resemble those of CPI, indicating strong structural homology. Amide proton exchange data of AVR9 and CPI are comparable (*10*, *26*). Thus, it is now firmly established that AVR9 is indeed a cystine-knotted peptide. Because of the structural homology to CPI, the solvent-accessible surfaces of the sulfur atoms involved in the bridging of CPI were examined (Figure 8). The sulfur atoms of the bridges Cys12−Cys27 and Cys18−Cys34 are not accessible to a TCEP molecule, whereas those of the bridge Cys8−Cys24 are sufficiently accessible. This perfectly rationalizes that only the bridge Cys2−Cys16 of AVR9 can be opened at relatively high TCEP concentrations. During reduction of the cystine-knotted trypsin inhibitor EETI II, only one intermediate was observed, which lacked the bridge between Cys2 and Cys19 (*33*, *34*). Also for this cystine knot, the bridge between the first and fourth cysteines is the only one accessible to reducing agents. This further supports that AVR9 is a cystine knot. Also, similarities in the folding of CPI (*35*), ω-conotoxins (*36*, *37*), and AVR9 (*13*) were observed. Possible relationships to other proteins come from a folding motif of CPI that was also identified in the cellulose-binding domain of fungal cellobiohydrolase I, wheat germ agglutinin, the erabutoxin family, and human neurophysin (*38*). A database search for cysteine patterns also indicated that an Amaranth α-amylase inhibitor, gurmarin (sweet taste-suppressing peptide), and antimicrobial peptides from *Amaranthus* are related to cystine-knotted peptides (*39*). Our recent query with the pattern x−C−x(2,6)−C−x(3,6)−C−x(2,5)−C−x(1,2)−C−x(3,6)−C−x (http://motif.genome.ad.jp/MOTIF2.html) resulted in peptide hits for 25 trypsin inhibitors, eight toxins, two carboxypeptidase inhibitors, and Kalata B1, but no new relevant sequences that are related to AVR9 were found.

The absence of obvious sequence identity to other structurally related peptides or proteins complicates the elucidation of the intrinsic function of AVR9. As this peptide is most homologous to CPI, we set out to test whether it possibly contained carboxypeptidase inhibiting activity. However, AVR9 did not inhibit the carboxypeptidase, not even at very high concentrations. Also, no antibacterial or antifungal activity could be detected for AVR9. This peptide was not active in an ω-conotoxin assay (David Craik, personal communication). It is, however, still possible that AVR9 displays an inhibitory or a channel-blocking activity in common with the related cystine-knotted peptides.

The elucidation of the bridging pattern of AVR9 provides a solid basis for the calculation of the 3D structure, thus gaining insight into the molecular mechanism underlying interaction with its (co)receptor and the subsequent onset of plant defense responses. This work is currently in progress.

ACKNOWLEDGMENT

The authors are most grateful to Ilse Landa (Laboratory of Biochemistry, Wageningen University, The Netherlands) for help with the carboxypeptidase inhibitor assay; to Fridolin van der Lecq (Sequence Center Utrecht, University of Utrecht, The Netherlands) for sequencing of the peptides; to Alejandro Perez Garcia (Laboratory of Phytopathology, Wageningen University, The Netherlands), Jannet Kamminga, and Wessel Lageweg (Zeneca Mogen, Leiden, The Netherlands) for help with the antibacterial and antifungal assays; and to David Craik (Centre for Drug Design and Development, University of Queensland, Australia) for performing ω-conotoxin assays.

REFERENCES

1. Flor, H. H. (1971) *Annu. Rev. Phytopathol. 9*, 275−296.
2. De Wit, P. J. G. M. (1997) *Trends Plant Sci. 2*, 452−458.
3. Joosten, M. H. A. J., and De Wit, P. J. G. M. (1999) *Annu. Rev. Phytopathol. 37*, 335−367.
4. Hammond-Kosack, K. E., and Jones, J. D. G. (1997) *Annu. Rev. Plant Physiol. Plant Mol. Biol. 48*, 575−607.
5. Scholtens-Toma, I. M. J., and De Wit, P. J. G. M. (1988) *Physiol. Mol. Plant Pathol. 33*, 59−67.
6. De Wit, P. J. G. M., Hofman, A. E., Velthuis, G. C. M., and Kuc, J. A. (1985) *Plant Physiol. 77*, 642−647.
7. Jones, D. A., Thomas, C. M., Hammond-Kosack, K. E., Balint-Kurti, P. J., and Jones, J. D. G. (1994) *Science 266*, 789−793.
8. De Wit, P. J. G. M. (1995) *Adv. Bot. Res. 21*, 147−185.
9. Crute, I. R., and Pink, D. A. C. (1996) *Plant Cell 8*, 1747−1755.
10. Vervoort, J., Van den Hooven, H. W., Berg, A., Vossen, P., Vogelsang, R., Joosten, M. H. A. J., and De Wit, P. J. G. M. (1997) *FEBS Lett. 404*, 153−158.
11. Kooman-Gersmann, M., Vogelsang, R., Hoogendijk, E. C. M., and De Wit, P. J. G. M. (1997) *Mol. Plant-Microbe Interact. 10*, 821−829.
12. Pallaghy, P. K., Nielsen, K. J., Craik, D. J., and Norton, R. S. (1994) *Protein Sci. 3*, 1833−1839.
13. Van den Hooven, H. W., Appelman, A. W. J., Zey, T., De Wit, P. J. G. M., and Vervoort, J. (1999) *Eur. J. Biochem. 264*, 9−18.
14. Hass, G. M., Nau, H., Biemann, K., Grahn, D. T., Ericsson, L. H., and Neurath, H. (1975) *Biochemistry 14*, 1334−1342.
15. Ryle, A. P., and Sanger, F. (1955) *Biochem. J. 60*, 535−540.
16. Zhou, Z., and Smith, D. L. (1990) *J. Protein Chem. 9*, 523−532.
17. Gray, W. R. (1993) *Protein Sci. 2*, 1732−1748.
18. Mahé, E., Vossen, P., Van den Hooven, H. W., Le-Nguyen, D., Vervoort, J., and De Wit, P. J. G. M. (1998) *J. Pept. Res. 52*, 482−494.
19. Henderson, P. J. F. (1972) *Biochem. J. 127*, 321−333.
20. Molina, M. A., Marino, C., Oliva, B., Avilés, F. X., and Querol, E. (1994) *J. Biol. Chem. 269*, 21467−21472.
21. Burns, J. A., Butler, J. C., Moran, J., and Whitesides, G. M. (1991) *J. Org. Chem. 56*, 2648−2650.
22. Wu, J., and Watson, J. T. (1997) *Protein Sci. 6*, 391−398.
23. Bures, E. J., Hui, J. O., Young, Y., Chow, D. T., Katta, V., Rohde, M. F., Zeni, L., Rosenfeld, R. D., Stark, K. L., and Haniu, M. (1998) *Biochemistry 37*, 12172−12177.
24. Young, Y., Zeni, L., Rosenfeld, R. D., Stark, K. L., Rohde, M. F., and Haniu, M. (1999) *J. Pept. Res. 54*, 514−521.
25. Hui, J. O., Le, J., Katta, V., Rohde, M. F., and Haniu, M. (1997) in *Techniques in Protein Chemistry VIII*, pp 277−287, Academic Press, San Diego.
26. Clore, G. M., Gronenborn, A. M., Nilges, M., and Ryan, C. A. (1987) *Biochemistry 26*, 8012−8023.
27. Hass, G. M., and Ryan, C. A. (1981) *Methods Enzymol. 80*, 778−791.
28. Heitz, A., Chiche, L., Le-Nguyen, D., and Castro, B. (1989) *Biochemistry 28*, 2392−2398.
29. Arai, K., Ishima, R., Morikawa, S., Miyasaka, A., Imoto, T., Yoshimura, S., Aimoto, S., and Akasaka, K. (1995) *J. Biomol. NMR 5*, 297−305.
30. Saether, O., Craik, D. J., Campbell, I. D., Sletten, K., Juul, J., and Norman, D. G. (1995) *Biochemistry 34*, 4147−4158.
31. Heck, S. D., Kelbaugh, P. R., Kelly, M. E., Thadeio, P. F., Saccomano, N. A., Stroh, J. G., and Volkmann, R. A. (1994) *J. Am. Chem. Soc. 116*, 10426−10436.
32. Price-Carter, M., Salem Hull, M., and Goldenberg, D. P. (1998) *Biochemistry 37*, 9851−9861.

33. Le-Nguyen, D., Heitz, A., Chiche, L., El Hajji, M., and Castro, B. (1993) *Protein Sci. 2*, 165−174.
34. Mahé, E., Le Nguyen, D., Heitz, A., Dafniet, R., Alfazema, L., Castro, B., and El Hajji, M. (1995) in *Proceedings of the 23rd European Peptide Symposium, September 4−10, 1995, Braga, Portugal* (Maia, H. L. S., Ed.) pp 422−423, ESCOM, Leiden.
35. Chang, J. Y., Canals, F., Schindler, P., Querol, E., and Avilés, F. X. (1994) *J. Biol. Chem. 269*, 22087−22094.
36. Price-Carter, M., Gray, W. R., and Goldenberg, D. P. (1996) *Biochemistry 35*, 15537−15546.
37. Price-Carter, M., Gray, W. R., and Goldenberg, D. P. (1996) *Biochemistry 35*, 15547−15557.
38. Holm, L., and Sander, C. (1993) *J. Mol. Biol. 233*, 123−138.
39. Chagolla-Lopez, A., Blanco-Labra, A., Patthy, A., Sánchez, R., and Pongor, S. (1994) *J. Biol. Chem. 269*, 23675−23680.
40. Wieczorek, M., Otlewski, J., Cook, J., Parks, K., Leluk, J., Wilimowska-Pelc, A., Polanowski, A., Wilusz, T., and Laskowski, M. (1985) *Biochem. Biophys. Res. Commun. 126*, 646−652.
41. Lew, M. J., Flinn, J. P., Pallaghy, P. K., Murphy, R., Whorlow, S. L., Wright, C. E., Norton, R. S., and Angus, J. A. (1997) *J. Biol. Chem. 272*, 12014−12023.
42. Rees, D. C., and Lipscomb, W. N. (1982) *J. Mol. Biol. 160*, 475−498.

BI0023089